

RESEARCH ARTICLE

Mechanism of Fat Mass and Obesity-Related Gene-Mediated Heme Oxygenase-1 m6A Modification in the Recovery of Neurological Function in Mice with Spinal Cord Injury

Jinghui Xu, MM , Zhenxiao Ren, MM, Tianzuo Niu, MM, Siyuan Li, MM

Department of Spine Surgery, The First Affiliated Hospital, Sun Yat-sen University (Guangdong Provincial Key Laboratory of Orthopaedics and Traumatology), Guangzhou, China

Objectives: This study examined the mechanism of fat mass and obesity-related gene (FTO)-mediated heme oxygenase-1 (HO-1) m6A modification facilitating neurological recovery in spinal cord injury (SCI) mice. FTO/HO-1 was identified as a key regulator of SCI as well as a potential target for treatment of SCI.

Methods: An SCI mouse was treated with pcDNA3.1-FTO/pcDNA3.1-NC/Dac51. An oxygen/glucose deprivation (OGD) cell model simulated SCI, with cells treated with pcDNA3.1-FTO/si-HO-1/Dac51. Motor function and neurobehavioral evaluation were assessed using the Basso, Beattie, and Bresnahan (BBB) scale and modified neurological severity score (mNSS). Spinal cord pathology and neuronal apoptosis were assessed. Further, FTO/HO-1 mRNA and protein levels, HO-1 mRNA stability, the interaction of YTHDF2 with HO-1 mRNA, neuronal viability/apoptosis, and HO-1 m6A modification were evaluated.

Results: Spinal cord injury mice exhibited reduced BBB, elevated mNSS scores, disorganized spinal cord cells, scattered nuclei, and severe nucleus pyknosis. pcDNA3.1-FTO elevated FTO mRNA, protein expression, and BBB score; reduced the mNSS score of SCI mice; decreased neuronal apoptosis; improved the cell arrangement; and improved nucleus pyknosis in spinal cord tissues. OGD decreased FTO expression. FTO upregulation ameliorated OGD-induced neuronal apoptosis. pcDNA3.1-FTO reduced HO-1 mRNA and protein and HO-1 m6A modification, while increasing HO-1 mRNA stability and FTO in OGD-treated cells. FTO upregulated HO-1 by modulating m6A modification. HO-1 downregulation attenuated the effect of FTO. pcDNA3.1-FTO/Dac51 increased the HO-1 m6A level in mouse spinal cord tissue homogenate, reduced BBB, boosted mNSS scores of SCI mice, aggravated nucleus pyknosis, and increased neuronal apoptosis in spinal cord tissues, confirming that FTO mediated HO-1 m6A modification facilitated neurological recovery in SCI mice.

Conclusion: The fat mass and obesity-related gene modulates HO-1 mRNA stability by regulating m6A modification levels, thereby influencing HO-1 expression and promoting neurological recovery in SCI mice.

Key words: Fat mass and obesity-related genes; HO-1; m6A; Neuron; Spinal cord injury

Introduction

Spinal cord injury (SCI) represents a prevalent form of neurotrauma resulting in sensory and motor dysfunction below the injured segment.¹ The molecular pathological

characteristics following SCI primarily involve an inflammatory response, oxidative stress, and heightened neuronal apoptosis.^{2,3} Presently, a definitive cure for SCI remains elusive, leaving patients subject to considerable physical and

Address for correspondence Jinghui Xu, Department of Spine Surgery, The First Affiliated Hospital, Sun Yat-sen University (Guangdong Provincial Key Laboratory of Orthopaedics and Traumatology), No. 58, Zhongshan Second Road, Yuexiu District, Guangzhou City, Guangdong Province, China, 510080; Tel: 86+18928807821 Email: xujh39@mail.sysu.edu.cn

Received 11 October 2023; accepted 4 January 2024

psychological pain. Moreover, the rising incidence of SCI places a substantial burden on patients, their families, and society as a whole.⁴ Despite some incremental progress in SCI treatment, achieving significant therapeutic breakthroughs remains a formidable challenge due to the intricate nature of its underlying mechanisms.⁵ Hence, rigorous investigation into the complex mechanisms underpinning SCI is imperative.

Heme oxygenase-1 (HO-1), a pivotal component within the heat shock protein family, intricately interfaces with cell anti-apoptotic and antioxidant defenses.⁶ Notably, inhibiting HO-1 expression using Zn-protoporphyrin effectively impedes TREM1-reduced inflammation and glial cell activation *in vitro*.⁷ Moreover, albumin demonstrates efficacy in ameliorating neuronal apoptosis and oxidative stress post-intracerebral hemorrhage in mice by upregulating HO-1 expression.⁸ Li et al. highlight the contributory role of the nuclear factor erythroid 2-related factor 2 (NRF2)/HO-1 pathway in functional recovery after SCI.⁹ N6-methyladenosine (m6A), a prevalent post-transcriptional modification in eukaryotic mRNAs, manifests significant enrichment in diverse regions, encompassing the coding sequence, the 5' untranslated region, 3' untranslated regions, and the termination codon.¹⁰ The m6A modification level exhibits a substantial increase in the oxygen/glucose deprivation (OGD) model in PC12 cells and SCI mice.¹¹ Fat mass and obesity-associated protein (FTO) is the first reported RNA N6-methyladenosine (m6A) demethylase in eukaryotic cells.¹² Silencing FTO elevates m6A modification levels, while FTO overexpression suppresses the m6A level.¹³ Notably, multiple studies have reported marked downregulation of FTO in SCI patients.^{14,15} Additionally, the m6A modification level undergoes a conspicuous elevation in the rat spinal cord hemisection and PC12 cells in the OGD model.¹¹ Various reader proteins, including IGF1BP3, YTHDC, and YTHDF, selectively recognize m6A modifications and regulate mRNA stability.¹⁵ Remarkably, YTHDF2 specifically binds to the m6A site, instigating the degradation of the complex by recruiting transcripts to the RNA.¹⁶ Additionally, ALKBH5 expression has been reported to attenuate m6A modification of FIP200 mRNA, resulting in diminished YTHDF2-mediated mRNA degradation and increased FIP200 levels, ultimately alleviating nucleus pulposus cells apoptosis.¹⁷ Interestingly, spinal nerve ligation enhances the binding of FTO to Mmp24 mRNA, facilitating MMP24 translation in the spinal cord, thereby contributing to the genesis of neuropathic pain.¹⁸ Therefore, we speculated that FTO might regulate the expression of HO-1, thereby affecting post-SCI neurological function recovery. However, the role and mechanism of FTO in the recovery of neurological function in SCI mice remain elusive. This study aims to (i) delve into the intricate mechanism of FTO-mediated HO-1 m6A modification; and (ii) shed light on FTO's potential in promoting neurological function recovery in SCI mice to provide novel insights for SCI treatment.

Materials and Methods

Ethics Statement

The study underwent a comprehensive review and obtained approval from the Animal Ethics Committee of The First Affiliated Hospital, Sun Yat-sen University (Guangdong Provincial Key Laboratory of Orthopedics and Traumatology) ([2023]010). We followed the approved protocol, with a strong emphasis on minimizing the number of animals used and alleviating their suffering.

Laboratory Animals

We obtained 72 female C57BL/6 mice aged 6–8 weeks and weighing 18–22 g from Vital River Laboratory Animal Technology in Beijing, China. They were housed in a specific pathogen-free standard animal facility, maintaining conditions at a temperature of $25 \pm 2^\circ\text{C}$, under a 12-h light/dark cycle and a relative humidity of $60\% \pm 5\%$. The mice had unrestricted access to both food and water.

Establishment of Spinal Cord Injury Mouse Model

We used a modified Allen method to establish the SCI model in C57BL/6 mice. Following intraperitoneal injection of pentobarbital sodium (1%, 80 mg/kg) for anesthesia, the mice underwent sterilization with iodophor. A longitudinal incision along the spine exposed the T9–T11 laminae. Subsequently, a laminectomy was performed at T10, and the spinal cord at T10 was impacted using a spinal cord percussion device (Model III, RWD, Shenzhen, Guangdong, China). The falling object weighed 5 g, with a diameter of 1.2 mm, and was impacted from a height of 50 mm. Post-surgery, mice were placed on cotton pads until fully recovered from anesthesia. Bladder emptying (three times a day) prevented urinary tract infection until spontaneous urination resumed. Mice received intraperitoneal injections of penicillin 100,000 U/time twice daily. The sham group ($N = 12$) underwent a similar surgical procedure, including a skin incision, but without related treatments or modeling surgery.

Animal Grouping and Treatment

Spinal cord injury mice were randomly allocated into six groups (12 mice/group): the sham group, the SCI group, the SCI + lentivirus (Lv)-oe-FTO group (mice were injected with pcDNA3.1-FTO Lv plasmid after SCI treatment), the SCI + Lv-oe-NC group (mice were treated with SCI and injected with pcDNA3.1-NC Lv plasmid), the SCI + Lv-oe-FTO + Dac51 group (mice were injected with pcDNA3.1-FTO Lv plasmid and Dac51 after SCI treatment), and the SCI + Lv-oe-FTO + dimethyl sulfoxide (DMSO) group (mice were treated with SCI and injected with pcDNA3.1-FTO Lv plasmid and equal amount of DMSO). Immediately post-injury, pcDNA3.1-FTO and pcDNA3.1-NC Lv ($2 \mu\text{L}$, 1×10^8 TU/mL, Hanbio, Shanghai, China) was injected into the lesion epicenter (depth of 0 to 0.5 mm) approximately 1 mm rostral and caudal. The

injection utilized a 10- μ L Hamilton syringe with a 32-G needle affixed to a micromanipulator. The needle advanced in 1- μ m increments, administering the virus at a rate of approximately 1 μ L/min and was held in position for 2–3 min to allow diffusion and prevent leakage or backflow.¹⁹ The FTO inhibitor Dac51 (20 mg/kg) (Abmole, Houston, TX, USA) was administered via tail vein injection. After behavioral experiments with 12 mice in each group, 48 mice were killed using a dose of 150 mg/kg sodium pentobarbital, and spinal cord tissues were promptly collected. Spinal cord tissues from six mice in each group were fixed with 4% paraformaldehyde, dehydrated, and embedded in paraffin for TdT-mediated dUTP-biotin nick end-labeling (TUNEL) and hematoxylin–eosin (HE) staining. Spinal cord tissues from the remaining six mice were processed into tissue homogenates and stored at -80°C for reverse transcription-quantitative polymerase chain reaction (RT-qPCR) and western blot assays.

Functional Behavior Assessments

Motor function in SCI mice was assessed using the Basso, Beattie, and Bresnahan (BBB) scale on days 3, 6, 14, 21, and 28 post-injury. Two investigators, unaware of group assignments to minimize bias, conducted the assessments. After allowing the mice to acclimate to the environment, locomotor function was observed and scored over a 5-min period by the experimenters. The scoring ranged from 0 to 21, where 0 points indicated hindlimb paralysis, 1–7 points reflected a limited range of motion in hindlimb joints, 8–13 points signified partial hindlimb mobility and walking ability, 14–20 points demonstrated fine motor skills using their paws, and 21 points represented normal motor function.

Neurobehavioral Assessment

The modified neurological severity score (mNSS) test was conducted on mice before the injury and on days 0, 7, 14, 21, and 28 post injury. This comprehensive test included evaluations of reflexes, sensation, and motor function. Scores for the test ranged from 0 to 18, with higher scores indicating more severe functional deficiency.

Hematoxylin–Eosin Staining

We prepared 5- μ m thick sections from the paraffin-embedded specimens of mouse spinal cord tissues. Tissue sections underwent deparaffinization using xylene and rehydration through a gradient of ethanol solutions. Subsequently, the sections were stained with HE staining solution (Solarbio, Beijing, China). The resulting pathological changes of spinal cord tissues were observed and documented under a light microscope (Olympus, Tokyo, Japan).

TUNEL Staining and Fluorescent Double-Labeling

After dewaxing the mouse spinal cord tissue sections with xylene and rehydrating them using a gradient of ethanol, we evaluated spinal cord tissue apoptosis using the TUNEL Apoptosis Detection Kit (Elabscience Biotechnology, Wuhan,

Hubei, China). Following TUNEL staining, sections were washed three times (5 min each) in tris-buffered saline (TBS), followed by incubation with mouse anti-NeuN (1:500, Chemicon, Temecula, CA, USA). After a TBS wash, the sections were treated with secondary antibodies (1:200; Alexa Fluor 594 donkey or anti-mouse, Molecular Probes, Eugene, OR, USA) for 1 h. We examined the sections under a fluorescence microscope (Zeiss, Oberkochen, Germany). In this analysis, normal cells displayed minimal fluorescence, while apoptotic cells (positive cells) emitted green fluorescence. To quantify apoptotic cells, we selected five fields (top, bottom, left, right, and center) on each slide for microscopic examination and calculated the percentage of apoptosis-positive cells in each field, determining the mean value.

Cell Culture and Establishment of Oxygen/Glucose Deprivation Model

Mouse spinal cord neurons primary cells MC178 were obtained from Yaji Biological (Shanghai, China) and were cultured at 37°C in high-glucose Dulbecco's modified Eagle's medium (DMEM; Thermo Fisher Scientific, Waltham, MA, USA) supplemented with 10% fetal bovine serum (Gibco, Grand Island, NY, USA) and 1% penicillin/streptomycin (Gibco) in a 5% CO_2 humidified atmosphere.

For the induction of OGD, mouse spinal cord neurons primary cells were seeded onto six-well plates (4×10^4 /well) pre-treated with 50 ng/mL nerve growth factor (NGF 2.5S, Invitrogen, Carlsbad, CA, USA). The six-well plates were incubated at 37°C for 72 h with 5% CO_2 . Subsequently, the culture medium was substituted with glucose-free DMEM (Gibco), and the cells were exposed to an anaerobic chamber with 94% N_2 /1% O_2 /5% CO_2 at 37°C for 4 h. Following this, the cells underwent two washes with Roswell Park Memorial Institute 1640 and were returned to normal medium for an additional 24 h.²⁰

The cells were divided into the following eight groups: the control group (normal culture), the OGD group (treated with OGD), the OGD + oe-FTO group (OGD-treated cells were transfected with pcDNA3.1-FTO), the OGD + oe-negative control (NC) group (OGD-treated cells were transfected with pcDNA3.1-NC), the OGD + oe-FTO + Dac51 group (OGD-treated cells were transfected with pcDNA3.1-FTO and added with 5 μ M Dac51 (FTO inhibitor),²¹ the OGD + oe-FTO + DMSO group (OGD-treated cells were transfected with pcDNA3.1-FTO and combined with an equal amount of DMSO as Dac51), the OGD + oe-FTO + si-HO-1 group (OGD-treated cells were transfected with pcDNA3.1-FTO and si-HO-1), and the OGD + oe-FTO + si-NC group (OGD-treated cells were transfected with pcDNA3.1-FTO and si-NC).

Cell transfections were conducted for 24 h using Lipofectamine 3000 (Invitrogen) at a final concentration of 3.75 μ L/mL.²² The transfection reagents used the encompassed pcDNA3.1-FTO and its NC pcDNA3.1-NC and si-HO-1 and its NC si-NC, all sourced from GenePharma (Shanghai, China).

RT-qPCR

Total RNA was extracted from spinal cord tissue homogenates or cells using TRIzol Reagent (Sigma-Aldrich St Louis, MO, USA). Complementary DNA was synthesized via reverse transcription using the PrimeScript™ RT Reagent Kit (TaKaRa, Kyoto, Japan). TaqMan primers and probes necessary for the assay were procured from TaKaRa. qPCR was conducted on an ABI 7500 (Applied Biosystem, Carlsbad, CA, USA) detection system. The reaction conditions involved an initial denaturation step at 95°C for 10 min, followed by 40 cycles of denaturation at 95°C for 10 s, annealing at 60°C for 20 s, and extension at 72°C for 34 s. The primer sequences are provided in Table 1. Each sample was analyzed in triplicate, and the relative expression of the target mRNA was determined using the $2^{-\Delta\Delta Ct}$ method, with glyceraldehyde-3-phosphate dehydrogenase (GAPDH) serving as the internal reference gene.

Western Blot

Spinal cord tissue homogenates or total cellular proteins were extracted using radio-immunoprecipitation assay cell lysis buffer (Beyotime, Nanjing, Jiangsu, China). Protein concentrations were determined with the Bicinchoninic Acid Protein Assay Kit (Beyotime). Subsequently, samples underwent 12% sodium dodecyl sulfate polyacrylamide gel electrophoresis (Thermo Fisher Scientific) for protein separation, followed by protein transfer onto polyvinylidene fluoride (PVDF) membranes via wet transfer (electrotransfer for 2 h in 70 V at 4°C in a cold room). The PVDF membrane was blocked in 5% skim milk-TBS with Tween 20 (TBST) and incubated at room temperature for 1 h. Next, the membrane was probed with specific primary antibodies (Abcam, Cambridge, UK) anti-FTO (1:1000, ab280081), anti-HO-1 (1:2000, ab189491), and anti-GAPDH (1:2500, ab9485) at 4°C overnight. Following incubation and TBST washing, the membranes were treated with horseradish peroxidase-labeled goat anti-rabbit secondary antibody immunoglobulin G (IgG; 1:2000, ab205718, Abcam) at room temperature for 1 h. Membranes were subjected to chemiluminescence for detection, and protein band density was quantified using the Image J software (National Institutes of Health, Bethesda,

Maryland, USA). GAPDH served as an internal reference, and each experiment was repeated three times.

3-(4, 5-Dimethylthiazol-2-Yl)-2, 5-Diphenyltetrazolium Bromide Assay

After removal of the cell culture medium, cells were incubated in a 5% CO₂ incubator at 37°C for 4 h, followed by an additional 4-h incubation with 20 µL of 3-(4, 5-dimethylthiazol-2-Yl)-2, 5-diphenyltetrazolium bromide (MTT) assay reagent (5 mg/mL; Thermo Fisher Scientific) at 37°C. Subsequently, 150 µL DMSO (20%) (Sigma-Aldrich) was added to dissolve the purple formazan crystals. The plate was then shaken for 10 min, and the absorbance was measured at 490 nm using a microplate spectrophotometer (Metsch Instruments, Shanghai, China). The cell survival rate of the control group was set at 100%, and the cell viability of each experimental group was determined as a ratio relative to its respective control group.

Flow Cytometry

To determine the apoptotic rate, we utilized the annexin V-fluorescein isothiocyanate/propidium iodide assay kit (BD Bioscience, San Jose, CA, USA). After two washes with phosphate-buffered saline, cells were stained in the dark at room temperature for 15 min. Subsequently, we assessed the apoptotic rate using flow cytometry (FACSCalibur, BD Bioscience) and analyzed the results with Flow Jo software (BD, Ashland, OR, USA).

Methylated RNA Immunoprecipitation

The SRAMP database (<http://www.cuilab.cn/sramp>) was used for predicting the m6A modification site on target RNA sequences. Total RNA was extracted using the TRIzol method, and purified mRNA was isolated using The Poly-A Tract mRNA Isolation Systems (A-Z5300; A&D Technology, Beijing, China). The immunoprecipitation (IP) buffer (140 mM NaCl, 20 mM Tris pH 7.5, 1% NP-40, 2 mM ethylene diamine tetra-acetic acid) was supplemented with anti-IgG antibody (1:100, ab109489, Abcam) or anti-m6A antibody (1:500, ab151230, Abcam). Subsequently, the antibody was co-cultivated with protein A/G magnetic beads for binding for 1 h. The magnetic bead-antibody complex and purified mRNA were added to IP buffer containing protease inhibitor and RNase inhibitor, and the sample was incubated at 4°C overnight. After elution with elution buffer, RNA was subjected to purification by phenol-chloroform extraction, and HO-1 analysis was performed through RT-qPCR.

RNA Stability

Following the inhibition of mRNA transcription using 5 µg/mL actinomycin D (MedChemExpress, Monmouth Junction, NJ, USA), cells were harvested at 0, 2, 4, and 6 h. Subsequently, mRNA levels were evaluated, and total RNA was extracted for RT-qPCR.

Table 1 Reverse transcription quantitative polymerase chain reaction primer sequences

Name of primer	Sequences (5'–3')
FTO (PMID: 37363723)	F:TGTCCTCAATGACTCAGACGATGG R:AGAACTGCCTCAGCCACTCAA
HO-1 (PMID: 35130906)	F:AAGCCGAGAATGCTGAGTTCA R:GCCGTGTAGATATGGTACAAGGA
GAPDH	F:GGTGGTCTCCTCTGACTTCAA R:GTTGCTGTAGCCAAATTCGTTGT

Abbreviations: FTO, fat mass and obesity-related genes; GAPDH, glyceraldehyde-3-phosphate dehydrogenase; HO-1, heme oxygenase-1.

Rip

Cell lysates were obtained using the Magna RIP Kit (Millipore, Billerica, MA, USA). Immunoprecipitation was performed with 50 μ L of protein A/G magnetic beads and 5 μ g of anti-YTHDF2 antibody (1:30, ab246514, Abcam), using normal rabbit IgG (1:100, ab172730, Abcam) as an NC. The captured RNA, after washing with RIP wash buffer, underwent qPCR analysis, and the data were normalized to calculate the relative expression.

Statistical Analysis

All data underwent statistical analysis and were graphed using GraphPad Prism 8.01 (GraphPad, San Diego, CA, USA). The data were presented as mean \pm standard deviation. The independent sample *t*-test was adopted for data comparisons between the two groups. Comparisons among multiple groups were assessed through one-way analysis of variance. Post hoc tests were subsequently conducted using Tukey's multiple comparisons test. Statistical significance was defined as a value of $p < 0.05$.

Results**Fat Mass and Obesity-Related Gene Inhibited Neuronal Apoptosis and Promoted the Recovery of Neurological Function in Spinal Cord Injury Mice**

We established the mouse SCI model for *in vivo* experiments based on Xu et al.²³ As presented in Figure 1A, mice were fully awake 2–3 h after surgery. Successful injury model establishment was confirmed by complete hind limb and tail paralysis, reduced muscle tension below the injury site, and lack of response to acupuncture and other stimuli. Motor function was assessed using BBB scores, and neurobehavioral evaluation was performed using mNSS. Our results showed significant reductions in BBB scores and increased mNSS scores compared to sham-operated mice (all $p < 0.001$) (Figure 1B,C). HE staining of spinal cord tissues from SCI mice revealed disorganized cells, scattered nuclei and severe nucleus pyknosis (Figure 1D). TUNEL staining co-labeled with the neuronal marker NeuN indicated a notable increase in TUNEL and NeuN co-positive cells in SCI mice compared to sham-operated mice ($p < 0.001$) (Figure 1E). RT-qPCR and western blot analyses showed a significant reduction in FTO mRNA and its protein expression in SCI mice compared to the sham-operated mice (all $p < 0.001$) (Figure 1F,G). Intrathecal injection of pcDNA3.1-FTO via lumbar puncture led to a substantial increase in FTO mRNA and protein expression in the spinal cord tissues of rats in the SCI + Lv-oe-FTO group. This increase was associated with improved BBB scores, reduced mNSS scores, a more orderly cellular arrangement, significant alleviation of nucleus pyknosis, and a remarkable decrease in TUNEL and NeuN co-positive cells compared to the SCI + Lv-oe-NC group (all $p < 0.01$) (Figure 1B–G). The results underscore the role of FTO in suppressing neuronal apoptosis and promoting the recovery of neurological function in SCI mice.

Oxygen/Glucose Deprivation Abated Fat Mass and Obesity-Related Gene Expression and Fat Mass and Obesity-Related Gene Upregulation Ameliorated**Oxygen/Glucose Deprivation-Caused Neuronal Apoptosis**

Primary cells of mouse spinal cord neurons subjected to OGD served as an *in vitro* cellular model of SCI, and cell experiments were performed (Figure 2A). The MTT assay revealed a significant decrease in neuronal viability in the OGD group relative to the control group ($p < 0.001$) (Figure 2B). Additionally, flow cytometry results highlighted a considerable increase in the neuronal apoptotic rate in the OGD group compared to the control group ($p < 0.001$) (Figure 2C). As demonstrated by RT-qPCR and western blot results, there was a marked reduction in FTO mRNA and protein expression levels in the OGD group compared to the control group (all $p < 0.001$) (Figure 2D,E). OGD-treated cells were subjected to transfection with either pcDNA3.1-FTO or pcDNA3.1-NC. Notably, the OGD + oe-FTO group exhibited significantly elevated FTO mRNA and protein expression patterns. Moreover, neuronal viability experienced a notable enhancement, and the apoptotic rate was markedly reduced compared to the OGD + oe-NC group (all $p < 0.05$) (Figure 2B–E). These findings indicate that OGD reduced FTO expression, and upregulating FTO could effectively alleviate OGD-induced neuronal apoptosis.

Fat Mass and Obesity-Related Gene Upregulated Heme Oxygenase-1 Expression by Modulating m6A Modification

Heme oxygenase-1 expression was assessed in cells through RT-qPCR and western blot analyses. The results revealed a significant reduction in both HO-1 mRNA and protein expression patterns following OGD (all $p < 0.001$) (Figure 3A,B). Conversely, in the GD + oe-FTO group, HO-1 mRNA and protein levels were upregulated compared to the OGD + oe-NC group (all $p < 0.05$) (Figure 3A,B). The SRAMP database predicted three m6A methylation modification sites on HO-1, which contained a high confidence binding site with a combined score of 0.654 (Figure 3C). To investigate the regulatory mechanism, we hypothesized that FTO might regulate HO-1 expression through the YTHDF2/m6A mRNA degradation pathway. Methylated RNA immunoprecipitation (Me-RIP) assay results provided strong evidence for this hypothesis, revealing that HO-1 m6A modification levels considerably increased in the OGD group compared with the control group but were distinctly inhibited in the OGD + oe-FTO group versus the OGD + oe-NC group (all $p < 0.001$) (Figure 3D). To evaluate the stability of HO-1 mRNA, we used the transcriptional inhibitor actinomycin D. Notably, HO-1 mRNA levels decreased over time. Importantly, HO-1 mRNA levels were lower in the OGD group than in the control group and higher in the OGD + oe-FTO group than in the OGD + oe-NC group at 2, 4, and 6 h after the addition of actinomycin D (all $p < 0.001$) (Figure 3E). Furthermore, RIP assays were conducted to investigate the interaction of

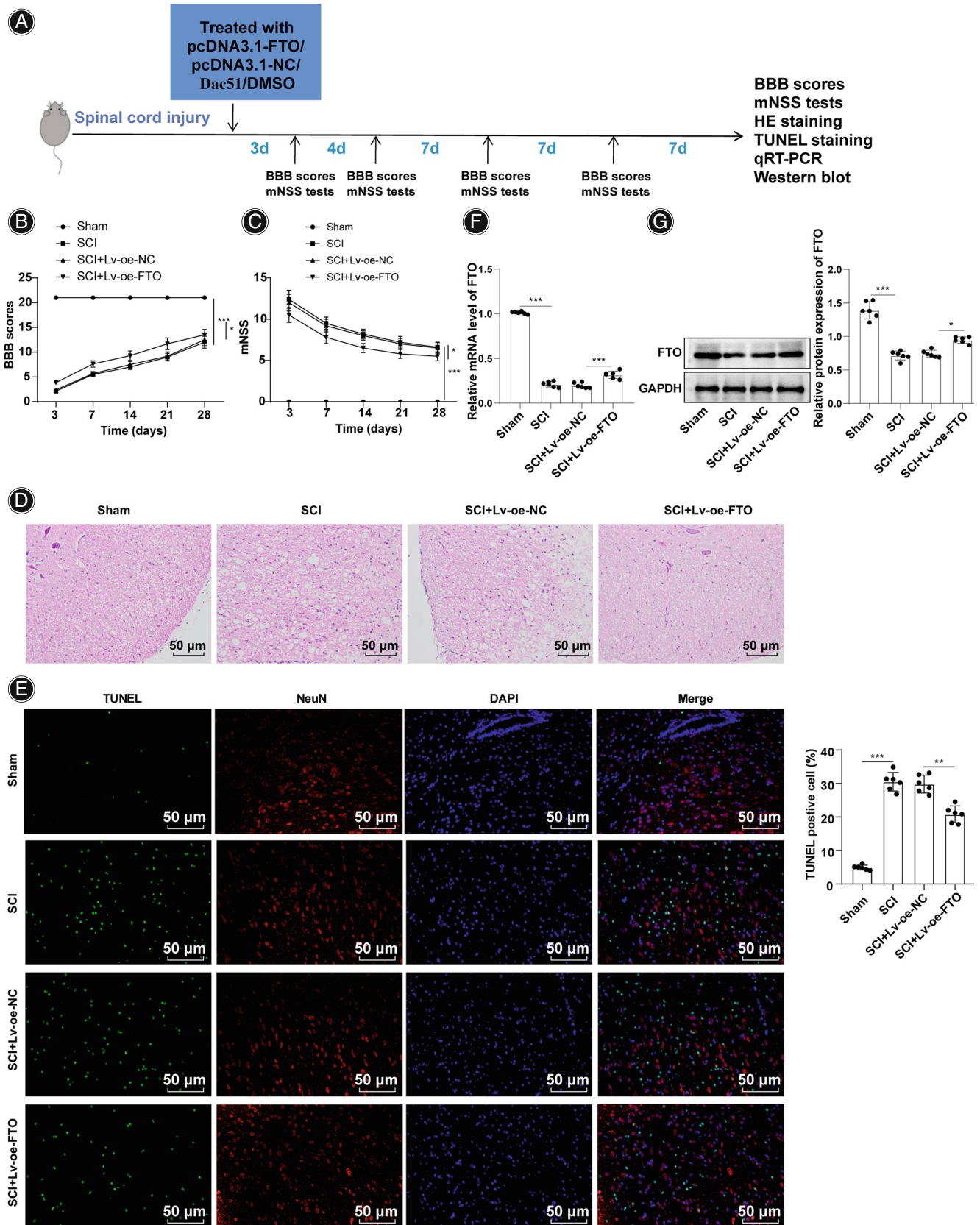


FIGURE 1 Legend on next page.

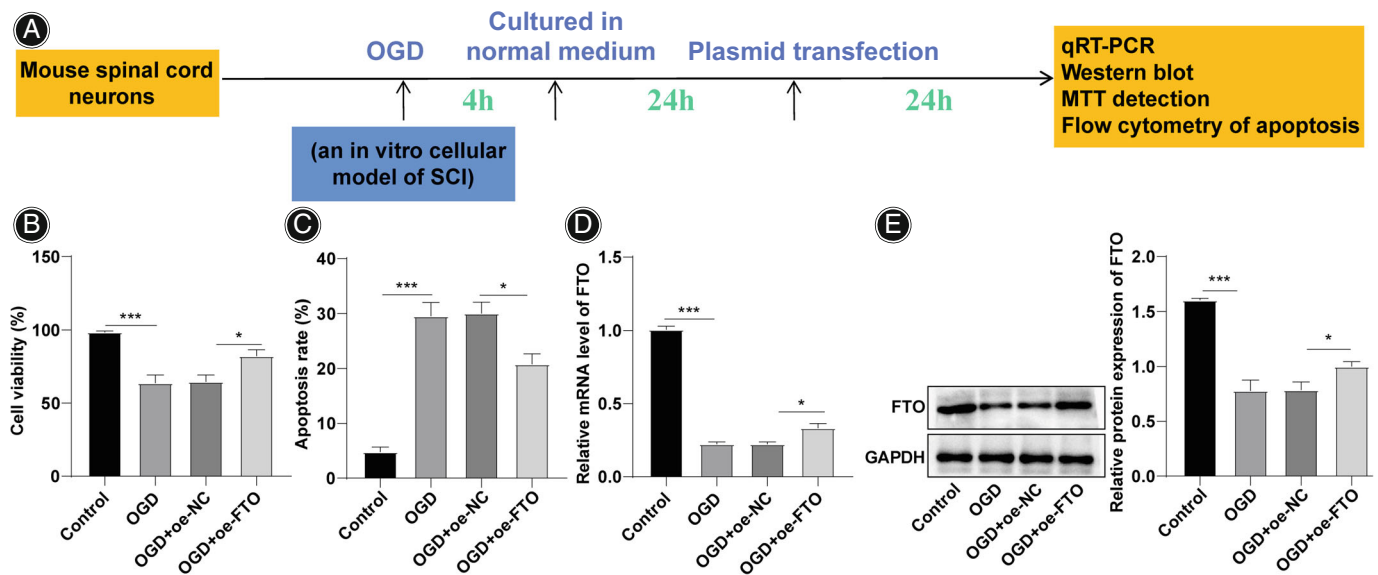


FIGURE 2 Oxygen/glucose deprivation (OGD) reduced fat mass and obesity-related genes (FTO) expression, and upregulation of FTO alleviated OGD-induced neuronal apoptosis. (A) Cell experiment scheme; (B) 2, 5-diphenyltetrazolium bromide (MTT) assay to assess neuronal viability; (C) flow cytometry to assess neuronal apoptosis; (D) reverse transcription-quantitative polymerase chain reaction (RT-qPCR) to measure FTO mRNA level; (E) and western blot to determine the FTO protein level. The cellular experiments were repeated three times, and the data were expressed as mean \pm standard deviation. One-way analysis of variance (ANOVA) was used to compare the data among multiple groups, and Tukey's multiple comparisons test was conducted for post hoc tests. * $p < 0.05$, *** $p < 0.001$.

YTHDF2 with HO-1, revealing the presence of interaction between YTHDF2 and HO-1 ($p < 0.001$) (Figure 3F). Subsequently, OGD-treated cells were transfected with pcDNA3.1-FTO and treated with 5 μ M FTO inhibitor Dac51. The HO-1 m6A modification level significantly increased in the OGD + oe-FTO + Dac51 group compared to the OGD + oe-FTO + DMSO group ($p < 0.05$) (Figure 3D), along with a decrease in HO-1 mRNA stability ($p < 0.001$) (Figure 3E) and downregulation of HO-1 mRNA and protein levels (all $p < 0.05$) (Figure 3A,B). In summary, these findings suggest that FTO upregulates HO-1 expression by modulating m6A modification.

Downregulation of Heme Oxygenase-1 Abated the Alleviating Effect of Fat Mass and Obesity-Related Gene on Oxygen/Glucose Deprivation-Induced Neuronal Apoptosis

In OGD-treated cells, simultaneous transfections of pcDNA3.1-FTO and si-HO-1 were conducted to suppress

HO-1 expression. The results showed a significant reduction in both HO-1 mRNA and protein levels. This reduction led to a notable decrease in neuronal viability and a distinct increase in the apoptotic rate in the OGD + oe-FTO + si-HO-1 group compared to the OGD + oe-FTO + si-NC group (all $p < 0.05$) (Figure 4A–D). The results demonstrated that the downregulation of HO-1 partially attenuated the protective effect of FTO against OGD-induced neuronal apoptosis.

Fat Mass and Obesity-Related Gene-Mediated Heme oxygenase-1 m6A Modification Promoted the Recovery of Neurological Function in Spinal Cord Injury Mice

To further verify that FTO-mediated HO-1 m6A modification contributes to the improvement in neurological function in SCI mice in vivo, we used Me-RIP to assess the HO-1 m6A modification level in mouse spinal cord tissue homogenates. The results revealed a notable increase in the HO-1 m6A level in spinal cord tissue homogenates of SCI mice

FIGURE 1 Fat mass and obesity-related genes (FTO) alleviated neuronal apoptosis and promoted neurological function recovery in SCI mice. (A) *In vivo* experimental scheme in mice. (B) Basso, Beattie, and Bresnahan (BBB) motor function scores, $N = 12$; (C) modified neurological severity score (mNSS) tests, $N = 12$; (D) hematoxylin–eosin (HE) staining to assess the pathological condition of spinal cord tissues, $N = 6$; (E) TdT-mediated dUTP-biotin nick end-labeling (TUNEL) staining to assess neuronal apoptosis in spinal cord tissues, $N = 6$; (F) reverse transcription-quantitative polymerase chain reaction (RT-qPCR) to determine FTO mRNA expression, $N = 6$; (G) western Blot to assess FTO protein expression, $N = 6$. Data were expressed as mean \pm standard deviation. One-way analysis of variance (ANOVA) was utilized for data comparisons among multiple groups. Tukey's multiple comparisons test was applied for post hoc test. * $p < 0.05$, ** $p < 0.01$, *** $p < 0.001$.

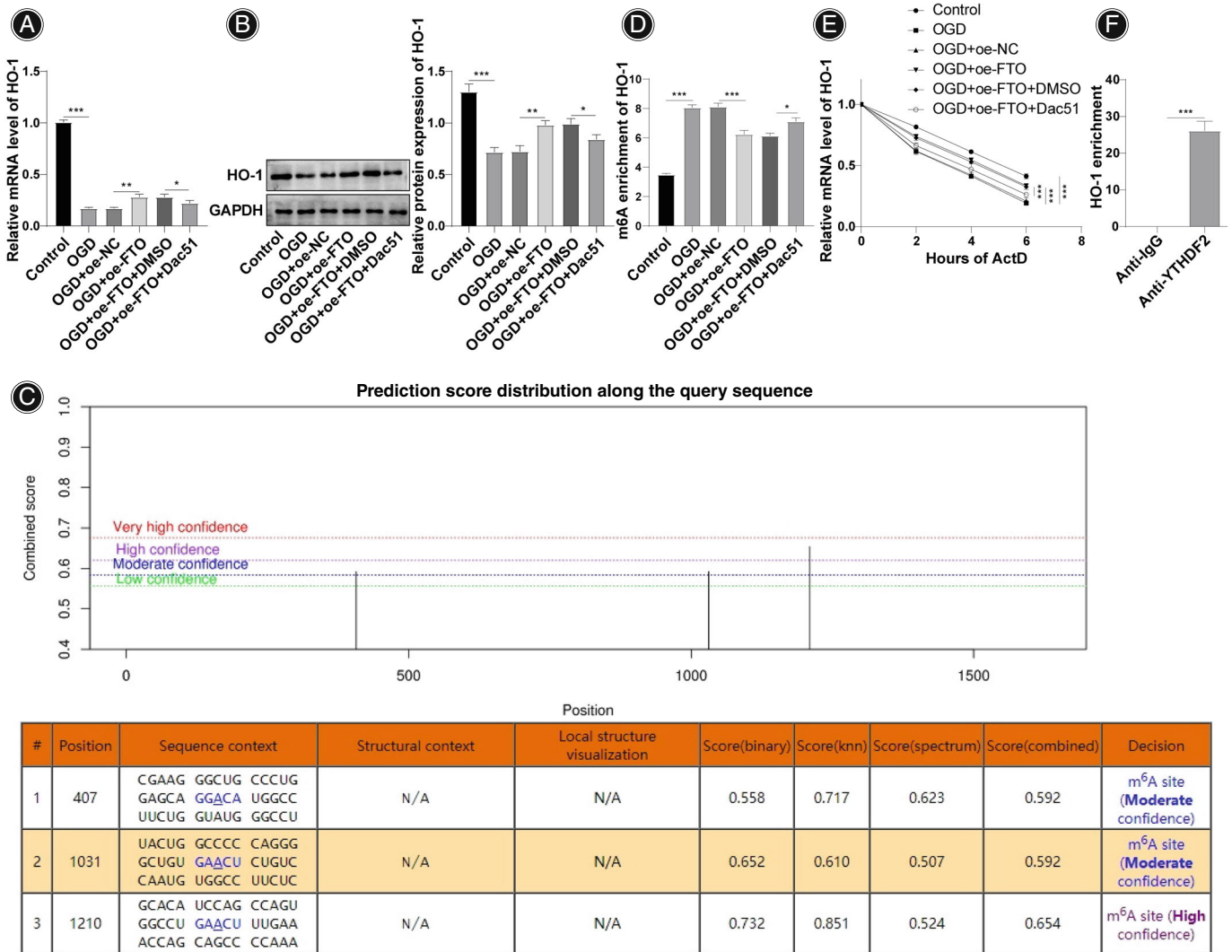


FIGURE 3 Fat mass and obesity-related genes (FTO) upregulated heme oxygenase-1 (HO-1) expression by modulating m⁶A modification. (A) Reverse transcription quantitative polymerase chain reaction (RT-qPCR) to measure HO-1 mRNA level; (B) western blot to determine HO-1 protein expression; (C) SRAMP database to predict m⁶A methylation modification sites on the HO-1 mRNA sequences; (D) methylated RNA immunoprecipitation (Me-RIP) assay to assess HO-1 m⁶A modification level; (E) actinomycin D to detect the stability of HO-1 mRNA in cells; (F) RIP to determine the interaction of YTHDF2 with HO-1. Cell experiments were repeated three times. Data were expressed as mean \pm standard deviation, and one-way analysis of variance (ANOVA) was implemented to compare data among multiple groups. Tukey's multiple comparisons test was used for post hoc tests. * $p < 0.05$, ** $p < 0.01$, *** $p < 0.001$.

compared to the mice in the sham group. However, in spinal cord tissue homogenates of the SCI + Lv-oe-FTO group, this level was markedly reduced relative to the SCI + Lv-oe-NC group (all $p < 0.01$) (Figure 5A). Following the injection of pcDNA3.1-FTO and Dac51 into mice, the results demonstrated a significant elevation in the HO-1 m⁶A level in spinal cord tissue homogenate in the SCI + Lv-oe-FTO + Dac51 group compared to the SCI + Lv-oe-FTO + DMSO group. Moreover, the SCI mice in the former group exhibited reduced BBB scores, elevated mNSS scores, more disordered cell arrangement, more serious nucleus

pyknosis, and increased TUNEL-positive cells (all $p < 0.05$) (Figure 5A–E). These findings underscore the pivotal role of FTO-mediated HO-1 m⁶A modification in promoting neurological function recovery in SCI mice.

Discussion

Spinal cord injury is a pervasive cause of disability and neurological dysfunction, with its global incidence steadily rising to approximately 15–40 cases per million people.²⁴ The condition is hallmarked by the loss of motor function, primarily attributed to neuronal apoptosis.²⁵ Apoptosis

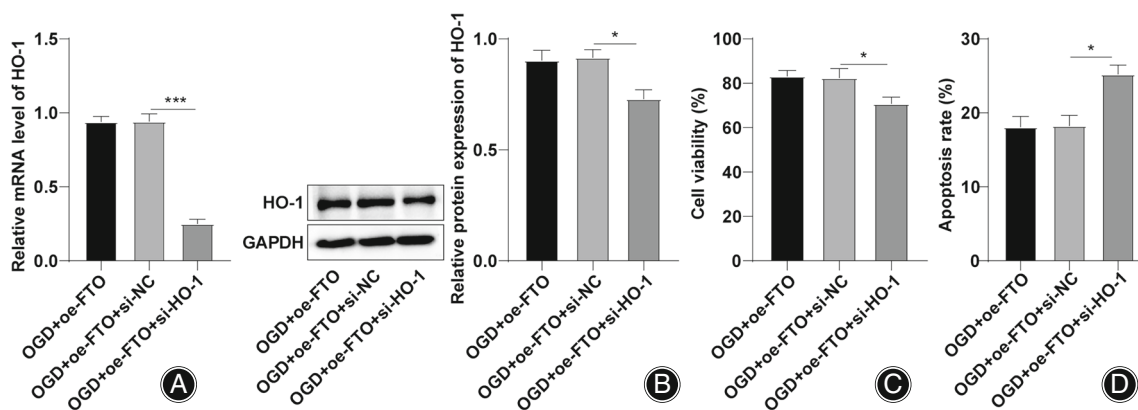


Figure 4 Heme oxygenase-1 (HO-1) knockdown partially reversed the suppressive effect of fat mass and obesity-related genes (FTO) on oxygen/glucose deprivation (OGD)-induced neuronal apoptosis. (A) Reverse transcription quantitative polymerase chain reaction (RT-qPCR) to assess HO-1 mRNA level; (B) western Blot to measure HO-1 protein level; (C) 2, 5-diphenyltetrazolium bromide (MTT) to evaluate neuronal viability; (D) flow cytometry to assess neuronal apoptosis. The cellular experiments were repeated three times. Data were expressed as mean \pm standard deviation, and one-way analysis of variance (ANOVA) was used to compare the data among multiple groups. Tukey's multiple comparisons test was used for post hoc test. * $p < 0.05$, *** $p < 0.001$.

induction further exacerbates SCI damage, ultimately progressing to irreversible injury and permanent paralysis.²⁶ Despite notable advancements in reducing SCI-related mortality, achieving substantial success in alleviating neurological injury has remained elusive.²⁷ Therefore, the restoration of neural function emerges as a paramount concern in the clinical management of SCI. Considering this imperative, our study sought to investigate strategies for enhancing neural function and curtailing neuronal apoptosis in SCI mice. Therefore, we successfully established the *in vivo* and *in vitro* models of SCI and explored the mechanism of FTO-mediated HO-1 m6A modification on spinal neuron apoptosis in neurological function recovery in SCI mice by overexpressing FTO.

Fat Mass and Obesity-Related Gene Facilitated Neurological Function Recovery in Spinal Cord Injury Mice

FTO has significant influences on neuronal development and the pathogenesis of various central nervous system diseases.^{28,29} Notably, the absence of FTO in the injured dorsal root ganglion has been demonstrated to reduce neuropathic pain in rats undergoing spinal nerve ligation.³⁰ Silencing FTO in neurons has been found to ameliorate cognitive deficits in mice exhibiting the symptoms of Alzheimer.³¹ Furthermore, Wang and colleagues reported distinct downregulation of FTO in SCI patients, suggesting FTO could potentially influence SCI through the induction of neuronal apoptosis.¹⁴ It has been documented that FTO is poorly expressed in spinal cord tissues and hypoxia-treated PC12 cells in contusion SCI rats, and FTO knockdown attenuates hypoxia-induced PC12 cell injury (PMID: 35803057). In line with previous studies, our study also revealed decreased FTO in SCI mice, and FTO overexpression

inhibited neuronal apoptosis, promoting neurological function recovery in SCI mice. Additionally, in an OGD scenario, FTO expression decreased, and FTO upregulation mitigated OGD-induced neuronal apoptosis. Similarly, the use of an FTO inhibitor enhanced dopamine neuron cell survival and suppressed apoptosis induced by growth factor deprivation.³² Upregulation of FTO also suppressed Nrf2 mRNA m6A methylation, leading to enhanced cell viability and reduced apoptosis in rats.³³

Fat Mass and Obesity-Related Gene-Mediated m6A Modification of Heme Oxygenase-1

m6A modification is a critical factor in various neuronal disorders and memory and learning processes.^{34,35} Following SCI, there are changes in the level of m6A modification, and RNA m6A modifications can influence cell death regulation, particularly neuronal apoptosis.³⁶ Elevated spinal cord m6A modification levels in chronic inflammatory pain mice and increased total RNA m6A levels in SCI rats have been observed.³⁷ Additionally, m6A modification levels are heightened in neurons in the OGD model of PC12 cells.¹¹ FTO, an RNA demethylase, exhibits an inverse relationship with m6A levels. FTO knockout enhances m6A modification levels, while FTO overexpression decreases them.¹³ HO-1, known for its protective role against inflammatory response, apoptosis, oxidative stress, and metabolic disorders,^{38,39} exhibits reduced levels in the spinal cord tissue of SCI mice.⁴⁰ Albumin has been reported to alleviate neurobehavioral deficits by upregulating HO-1 expression after intracerebral hemorrhage.⁸ Our study explores how FTO influences SCI through m6A modification. Innovatively, our study revealed that FTO upregulates HO-1 expression by modulating m6A modification after OGD. FTO-mediated HO-1 m6A modification plays a pivotal role in promoting neurological function

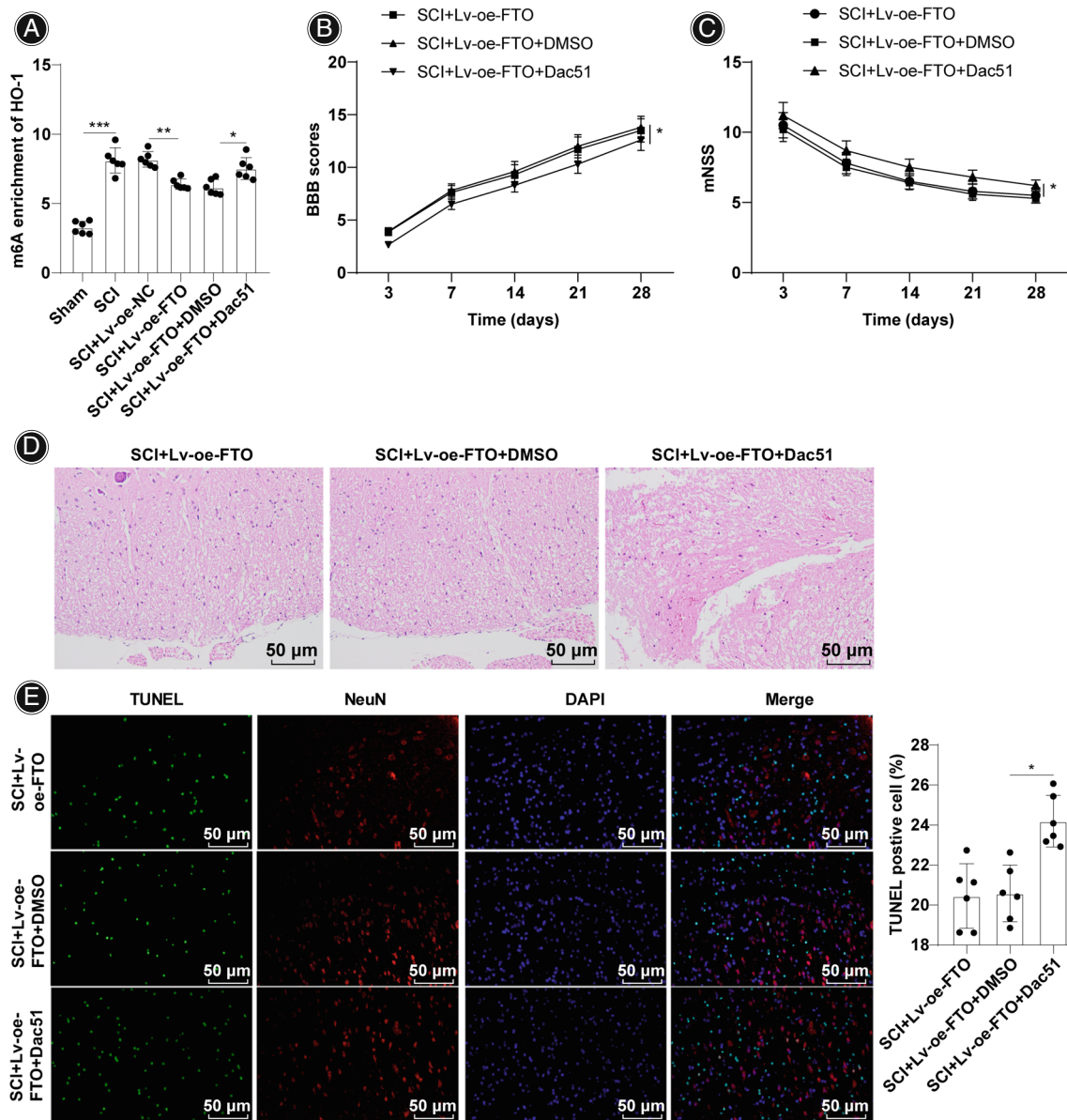


Figure 5 Fat mass and obesity-related genes (FTO)-mediated heme oxygenase-1 (HO-1) m6A modification facilitated neurological function recovery in spinal cord injury (SCI) mice. (A) Methylated RNA immunoprecipitation (Me-RIP) to test HO-1 m6A modification level in mouse spinal cord tissue homogenate, $N = 6$; (B) Basso, Beattie, and Bresnahan (BBB) motor function score, $N = 12$; (C) modified neurological severity score (mNSS) tests, $N = 12$; (D) hematoxylin–eosin staining to assess the pathological condition of spinal cord tissue, $N = 6$; (E) TdT-mediated dUTP-biotin nick end-labeling (TUNEL) staining to evaluate apoptosis in spinal cord tissues, $N = 6$. Data were expressed as mean \pm standard deviation. One-way analysis of variance (ANOVA) was applied for comparisons of data among multiple groups, and Tukey's multiple comparisons test was used for post hoc tests. * $p < 0.05$, ** $p < 0.01$, *** $p < 0.001$.

recovery in SCI mice. Additionally, the downregulation of HO-1 partially reversed the beneficial effects of FTO on OGD-induced neuronal apoptosis. Exogenous HO-1 has been shown to reduce SCI-induced neuronal apoptosis and enhance neurological scores.⁴¹ Consistent with our study, a prior study revealed that activation of the Nrf2/HO-1 pathway suppresses neuronal apoptosis and alleviates oxidative stress in SCI rats,⁴² facilitating functional recovery in mice

with SCI.⁴³ Importantly, prior research highlights the synergistic effects of the HO-1 pathway and PPAR α agonists in enhancing motor function and mitigating SCI in SCI rats.⁴⁴

Limitations and Strengths

However, a notable limitation is the minimal exploration of FTO's downstream targets and specific pathways of action, a focus for future research. Due to constraints in laboratory

conditions and funding, electromyography data is currently unavailable. Future studies aim to expand our investigation into SCI.

This study is the first to explore how FTO represses neuronal apoptosis and promotes neurological function recovery in SCI mice. Further, this study is the first to examine how FTO upregulates HO-1 expression by modulating m6A modification to alleviate OGD-induced neuronal apoptosis. Finally, this study verified *in vivo* in animals that FTO mediated HO-1 m6A modification to facilitate neurological function recovery in SCI mice, thus offering new insight for the treatment of SCI.

Conclusion

In summary, our findings highlight FTO's influence on HO-1 mRNA stability by regulating m6A modification levels, affecting HO-1 expression and contributing to the enhanced neurological function recovery in SCI mice. Our study presents innovative strategies for the treatment of SCI.

Author Contributions

All authors contributed to the study conception and design, and all authors commented on previous versions of the manuscript. All authors read and approved the final manuscript. All persons designated as authors qualify for authorship, and all those who qualify for authorship are listed. J.X. was responsible for the integrity assurance of the entire research, the definition of knowledge content and literature research, experimental research, data analysis, manuscript preparation and manuscript editing. Z.R. was

responsible for ensuring the integrity of the entire research and the definition of the knowledge content. He contributed to the literature research, experimental research, and statistical analysis. T.N. contributed to the data acquisition and provided clinical studies. S.L. was responsible for study concepts, study design, and manuscript review.

Acknowledgements

This research received no external funding.

Conflict of Interest Statement

The authors declare that the research was conducted in the absence of any commercial or financial relationships that could be construed as a potential conflict of interest. The authors declare no conflicts of interest.

Ethics Statement

The study underwent a comprehensive review and received approval from the Animal Ethics Committee of The First Affiliated Hospital, Sun Yat-sen University (Guangdong Provincial Key Laboratory of Orthopedics and Traumatology) ([2023]010). We strictly adhered to the approved protocol, placing significant emphasis on reducing the number of animals used and mitigating their suffering.

Data Availability Statement

The data that support the findings of this study are available from the corresponding author upon reasonable request.

References

1. Quadri SA, Farooqui M, Ikram A, Zafar A, Khan MA, Suriya SS, et al. Recent update on basic mechanisms of spinal cord injury. *Neurosurg Rev.* 2020;43(2):425–41.
2. He N, Zheng X, He T, Shen G, Wang K, Hu J, et al. MCC950 reduces neuronal apoptosis in spinal cord injury in mice. *CNS Neurol Disord Drug Targets.* 2021;20(3):298–308.
3. Rong Y, Ji C, Wang Z, Ge X, Wang J, Ye W, et al. Correction to: small extracellular vesicles encapsulating CCL2 from activated astrocytes induce microglial activation and neuronal apoptosis after traumatic spinal cord injury. *J Neuroinflammation.* 2021;18(1):285.
4. Fan B, Wei Z, Yao X, Shi G, Cheng X, Zhou X, et al. Microenvironment imbalance of spinal cord injury. *Cell Transplant.* 2018;27(6):853–66.
5. Anjum A, Yazid MD, Fauzi Daud M, Idris J, Ng AMH, Selvi Naicker A, et al. Spinal cord injury: pathophysiology, multimolecular interactions, and underlying recovery mechanisms. *Int J Mol sci.* 2020;21(20):7533.
6. Wang Y, Yang C, Elsheikh NAH, Li C, Yang F, Wang G, et al. HO-1 reduces heat stress-induced apoptosis in bovine granulosa cells by suppressing oxidative stress. *Aging (Albany NY).* 2019;11(15):5535–47.
7. Li Z, Wu F, Xu D, Zhi Z, Xu G. Inhibition of TREM1 reduces inflammation and oxidative stress after spinal cord injury (SCI) associated with HO-1 expressions. *Biomed Pharmacother.* 2019;109:2014–21.
8. Deng S, Liu S, Jin P, Feng S, Tian M, Wei P, et al. Albumin reduces oxidative stress and neuronal apoptosis via the ERK/Nrf2/HO-1 pathway after intracerebral hemorrhage in rats. *Oxid Med Cell Longev.* 2021;2021:8891373.
9. Li D, Tian H, Li X, Mao L, Zhao X, Lin J, et al. Zinc promotes functional recovery after spinal cord injury by activating Nrf2/HO-1 defense pathway and inhibiting inflammation of NLRP3 in nerve cells. *Life sci.* 2020;245:117351.
10. Ran Y, Yan Z, Huang M, Zhou S, Wu F, Wang M, et al. Severe burn injury significantly alters the gene expression and m6A methylation tagging of mRNAs and lncRNAs in human skin. *J Pers Med.* 2023;13(1):150.
11. Guo S, Lin T, Chen G, Shangguan Z, Zhou L, Chen Z, et al. METTL3 affects spinal cord neuronal apoptosis by regulating Bcl-2 m6A modifications after spinal cord injury. *Neurospine.* 2023;20(2):623–36.
12. Azzam SK, Alsafar H, Sajini AA. FTO m6A demethylase in obesity and cancer: implications and underlying molecular mechanisms. *Int J Mol sci.* 2022;23(7):3800.
13. Jia G, Fu Y, Zhao X, Dai Q, Zheng G, Yang Y, et al. N6-methyladenosine in nuclear RNA is a major substrate of the obesity-associated FTO. *Nat Chem Biol.* 2011;7(12):885–7.
14. Wang D, Li Y, Xu X, Zhao S, Wang Z, Yang J, et al. FTO knockdown alleviates hypoxia-induced PC12 cell injury by stabilizing GADD45B in an IGF2BP2-dependent manner. *Biochem Biophys Res Commun.* 2022;619:166–72.
15. Liang Y, Han H, Xiong Q, Yang C, Wang L, Ma J, et al. METTL3-mediated m(6)A methylation regulates muscle stem cells and muscle regeneration by notch signaling pathway. *Stem Cells Int.* 2021;2021:9955691.
16. Wang X, Lu Z, Gomez A, Hon GC, Yue Y, Han D, et al. N6-methyladenosine-dependent regulation of messenger RNA stability. *Nature.* 2014;505(7481):117–20.
17. Li G, Song Y, Liao Z, Wang K, Luo R, Lu S, et al. Bone-derived mesenchymal stem cells alleviate compression-induced apoptosis of nucleus pulposus cells by N6 methyladenosine of autophagy. *Cell Death Dis.* 2020;11(2):103.
18. Ma L, Huang Y, Zhang F, Gao DS, Sun N, Ren J, et al. MMP24 contributes to neuropathic pain in an FTO-dependent manner in the spinal cord neurons. *Front Pharmacol.* 2021;12:673831.
19. Patel M, Li Y, Anderson J, Castro-Pedrido S, Skinner R, Lei S, et al. Gsx1 promotes locomotor functional recovery after spinal cord injury. *Mol Ther.* 2021;29(8):2469–82.
20. Lin T, Zhao Y, Guo S, Wu Z, Li W, Wu R, et al. Apelin-13 protects neurons by attenuating early-stage Postspinal cord injury apoptosis in vitro. *Brain sci.* 2022;12(11):1515.
21. Liu Y, Liang G, Xu H, Dong W, Dong Z, Qiu Z, et al. Tumors exploit FTO-mediated regulation of glycolytic metabolism to evade immune surveillance. *Cell Metab.* 2021;33(6):1221–33.
22. Zietzer A, Hosen MR, Wang H, Goody PR, Sylvester M, Latz E, et al. The RNA-binding protein hnRNPU regulates the sorting of microRNA-30c-5p into large extracellular vesicles. *J Extracell Vesicles.* 2020;9(1):1786967.

- 23.** Xu S, Wang J, Jiang J, Song J, Zhu W, Zhang F, et al. TLR4 promotes microglial pyroptosis via lncRNA-F63002801ORik by activating PI3K/AKT pathway after spinal cord injury. *Cell Death Dis.* 2020;11(8):693.
- 24.** Fan L, Li X, Liu T. Asiaticoside inhibits neuronal apoptosis and promotes functional recovery after spinal cord injury in rats. *J Mol Neurosci.* 2020;70(12):1988–96.
- 25.** Wang J, Zhao W, Wang X, Gao H, Liu R, Shou J, et al. Enhanced store-operated calcium entry (SOCE) exacerbates motor neurons apoptosis following spinal cord injury. *Gen Physiol Biophys.* 2021;40(1):61–9.
- 26.** Kiehn O. Decoding the organization of spinal circuits that control locomotion. *Nat Rev Neurosci.* 2016;17(4):224–38.
- 27.** Varma A, Hill EG, Nicholas J, Selassie A. Predictors of early mortality after traumatic spinal cord injury: a population-based study. *Spine (Phila Pa 1976).* 2010;35(7):778–83.
- 28.** Annapoorna PK, Iyer H, Parnaik T, Narasimhan H, Bhattacharya A, Kumar A. FTO: an emerging molecular player in neuropsychiatric diseases. *Neuroscience.* 2019;418:15–24.
- 29.** Chen X, Yu C, Guo M, Zheng X, Ali S, Huang H, et al. Down-regulation of m6A mRNA methylation is involved in dopaminergic neuronal death. *ACS Chem Neurosci.* 2019;10(5):2355–63.
- 30.** Li Y, Guo X, Sun L, Xiao J, Su S, Du S, et al. N(6)-Methyladenosine demethylase FTO contributes to neuropathic pain by stabilizing G9a expression in primary sensory neurons. *Adv sci (Weinh).* 2020;7(13):1902402.
- 31.** Li H, Ren Y, Mao K, Hua F, Yang Y, Wei N, et al. FTO is involved in Alzheimer's disease by targeting TSC1-mTOR-tau signaling. *Biochem Biophys Res Commun.* 2018;498(1):234–9.
- 32.** Selberg S, Yu LY, Bondarenko O, Kankuri E, Seli N, Kovaleva V, et al. Small-molecule inhibitors of the RNA m6A demethylases FTO potently support the survival of dopamine neurons. *Int J Mol Sci.* 2021;22(9):4537.
- 33.** Tian MQ, Li J, Shu XM, Lang CH, Chen J, Peng LY, et al. The increase of Nrf2 m6A modification induced by FTO downregulation promotes hippocampal neuron injury and aggravates the progression of epilepsy in a rat model. *Synapse.* 2023;77(4):e22270.
- 34.** Satterlee JS, Basanta-Sanchez M, Blanco S, Li JB, Meyer K, Pollock J, et al. Novel RNA modifications in the nervous system: form and function. *J Neurosci.* 2014;34(46):15170–7.
- 35.** Zhang C, Wang Y, Peng Y, Xu H, Zhou X. METTL3 regulates inflammatory pain by modulating m(6)A-dependent pri-miR-365-3p processing. *FASEB J.* 2020;34(1):122–32.
- 36.** Liu D, Fan B, Li J, Sun T, Ma J, Zhou X, et al. N6-methyladenosine modification: a potential regulatory mechanism in spinal cord injury. *Front Cell Neurosci.* 2022;16:989637.
- 37.** Wang H, Yuan J, Dang X, Shi Z, Ban W, Ma D. Mettl14-mediated m6A modification modulates neuron apoptosis during the repair of spinal cord injury by regulating the transformation from pri-mir-375 to miR-375. *Cell Biosci.* 2021;11(1):52.
- 38.** Dwivedi S, Rajasekar N, Hanif K, Nath C, Shukla R. Sulforaphane ameliorates okadaic acid-induced memory impairment in rats by activating the Nrf2/HO-1 antioxidant pathway. *Mol Neurobiol.* 2016;53(8):5310–23.
- 39.** Wang L, Yao Y, He R, Meng Y, Li N, Zhang D, et al. Methane ameliorates spinal cord ischemia-reperfusion injury in rats: antioxidant, anti-inflammatory and anti-apoptotic activity mediated by Nrf2 activation. *Free Radic Biol Med.* 2017;103:69–86.
- 40.** Zhang X, Xu L, Chen X, Zhou X, Cao L. Acacetin alleviates neuroinflammation and oxidative stress injury via the Nrf2/HO-1 pathway in a mouse model of spinal cord injury. *Transl Neurosci.* 2022;13(1):483–94.
- 41.** Lin W, Wang S, Yang Z, Lin J, Ke Q, Lan W, et al. Heme Oxygenase-1 inhibits neuronal apoptosis in spinal cord injury through Down-regulation of Cdc42-MLK3-MKK7-JNK3 Axis. *J Neurotrauma.* 2017;34(3):695–706.
- 42.** Lv R, Du L, Zhang L, Zhang Z. Polydatin attenuates spinal cord injury in rats by inhibiting oxidative stress and microglia apoptosis via Nrf2/HO-1 pathway. *Life sci.* 2019;217:119–27.
- 43.** Gong F, Ge T, Liu J, Xiao J, Wu X, Wang H, et al. Trehalose inhibits ferroptosis via NRF2/HO-1 pathway and promotes functional recovery in mice with spinal cord injury. *Aging (Albany NY).* 2022;14(7):3216–32.
- 44.** Zhang H, Xiang D, Liu X, Xiang L. PPARalpha agonist relieves spinal cord injury in rats by activating Nrf2/HO-1 via the Raf-1/MEK/ERK pathway. *Aging (Albany NY).* 2021;13(22):24640–54.